Journal of proteome research

Article

pubs.acs.org/jpr

Urinary Metabolic Phenotyping the slc26a6 (Chloride–Oxalate Exchanger) Null Mouse Model

Isabel Garcia-Perez,[⊥,†,§,▽] Alma Villaseñor,[⊥,‡] Anisha Wijeyesekera,[†,▽] Joram M. Posma,[†,§,▽] Zhirong Jiang,[¶] Jeremiah Stamler,[∥] Peter Aronson,[¶] Robert Unwin,[#] Coral Barbas,[‡] Paul Elliott,[§,▽] Jeremy Nicholson,[⊥,†,▽] and Elaine Holmes*[,⊥,†,▽]

[†]Biomolecular Medicine, Department of Surgery and Cancer, Faculty of Medicine, Imperial College London, SW7 2AZ, London, U.K.

[‡]CEMBIO (Center for Metabolomics and Bioanalysis) Pharmacy Faculty, Campus Monteprincipe, Universidad CEU San Pablo, Madrid, Spain

[§]Department of Epidemiology and Biostatistics, School of Public Health, Faculty of Medicine, Imperial College London, London, U.K.

[∥]Department of Preventive Medicine, Feinberg School of Medicine, Northwestern University, Chicago, Illinois, United States

[¶]Department of Internal Medicine, Yale University School of Medicine, New Haven, Connecticut, United States

[#]UCL Centre for Nephrology, Royal Free Hospital, University College London, London, U.K.

[▽]MRC-HPA Centre for Environment and Health, Imperial College London, London, U.K.

Supporting Information

ABSTRACT: The prevalence of renal stone disease is increasing, although it remains higher in men than in women when matched for age. While still somewhat controversial, several studies have reported an association between renal stone disease and hypertension, but this may be confounded by a shared link with obesity. However, independent of obesity, hyperoxaluria has been shown to be associated with hypertension in stone-formers, and the most common type of renal stone is composed of calcium oxalate. The chloride–oxalate exchanger slc26a6 (also known as CFEX or PAT-1), located in the renal proximal tubule, was originally thought to have an important role in sodium homeostasis and thereby blood pressure control, but it has recently been shown to have a key function in oxalate balance by mediating oxalate secretion in the gut. We have applied two orthogonal analytical platforms (NMR spectroscopy and capillary electrophoresis with UV detection) in parallel to characterize the urinary metabolic signatures related to the loss of the renal chloride–oxalate exchanger in slc26a6 null mice. Clear metabolic differentiation between the urinary profiles of the slc26a6 null and the wild type mice were observed using both methods, with the combination of NMR and CE-UV providing extensive coverage of the urinary metabolome. Key discriminating metabolites included oxalate, *m*-hydroxyphenylpropionylsulfate (*m*-HPPS), trimethylamine-*N*-oxide, glycolate and *scyllo*-inositol (higher in slc26a6 null mice) and hippurate, taurine, trimethylamine, and citrate (lower in slc26a6 null mice). In addition to the reduced efficiency of anion transport, several of these metabolites (hippurate, *m*-HPPS, methylamines) reflect alteration in gut microbial cometabolic activities. Gender-related metabotypes were also observed in both wild type and slc26a6 null groups. Urinary metabolites that showed a sex-specific pattern included trimethylamine, trimethylamine-*N*-oxide, citrate, spermidine, guanidinoacetate, and 2-oxoisocaproate. The gender-dependent metabolic expression of the consequences of slc26a6 deletion might have relevance to the difference in prevalence of renal stone formation in men and women. The different composition of microbial metabolites in the slc26a6 null mice is consistent with the fact that the slc26a6 transporter is found in a range of tissues, including the kidney and intestine, and provides further evidence for the "long reach" of the microbiota in physiological and pathological processes.

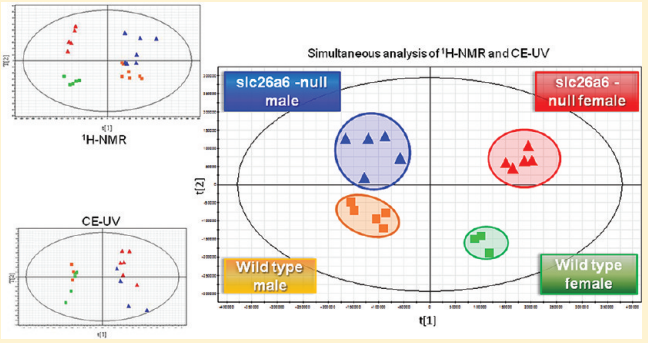

KEYWORDS: *oxalate, slc26a6, CFEX, NMR spectroscopy, metabolic profiling, capillary electrophoresis*

INTRODUCTION

There is an epidemiological association between renal stone formation and other disorders such as hypertension,[1,2] type 2 diabetes, and obesity. However, the mechanistic and aeitopathogenic links between these apparently diverse conditions are not fully understood.[1] The most common stone type is composed of calcium oxalate, and for this reason, there has always been interest in oxalate metabolism and excretion in renal stone disease. An animal model that has shed light on the importance of altered oxalate balance in renal stone formation is the slc26a6 (CFEX, PAT-1) null mouse, originally produced because of

Received: December 22, 2011
Published: May 17, 2012

dx.doi.org/10.1021/pr2012544 | *J. Proteome Res.* 2012, 11, 4425–4435

the expression of this chloride−oxalate (formate) exchanger in the renal proximal tubule, and a postulated role in renal sodium reabsorption and thus blood pressure control.[3,4] Moreover, a large-scale metabolome-wide association study found an inverse correlation between urinary formate levels and diastolic blood pressure.[5] However, to date there is no clear evidence for a direct link between the function of this exchanger and blood pressure. Indeed, slc26a6 has a broad specificity, and in addition to oxalate and formate, it can also transport chloride, sulfate and bicarbonate; transport is also inhibited by *p*-aminohippurate.[7] This transporter is not found exclusively in the kidney, but it is also present in the gut (small intestine, cecum, and proximal colon), pancreas, skeletal muscle, and heart.[3] However, its highest affinity is for oxalate, which has been the main focus of recent attention, prompted by the serendipitous finding of calcium oxalate renal stone formation in slc26a6 null mice due to significant hyperoxaluria secondary to reduced gut secretion of oxalate, leading to increased circulating levels.[3]

A dual metabolic profiling strategy, combining NMR spectroscopy with CE-UV of the same urine sample, has been applied in order to comprehensively describe the urinary metabolic phenotype of the slc26a6-null mouse model. Both technologies have been widely applied in the metabolic fingerprinting of various diseases, including hypertension, type 2 diabetes, and inflammatory conditions, and together offer complementary information. While NMR generates comprehensive and robust profiles of a broad range of low molecular weight molecules, CE-UV can provide quantitative data on ionic species including chloride and nitrates. Here we show the direct relationship between urinary oxalate and a range of urinary metabolites and show clear sex-dependent slc26a6-related differences in metabolism.

MATERIALS AND METHODS

Sample Collection

Urine samples were provided by the Department of Internal Medicine, Yale University School of Medicine. Wild type control and slc26a6 null mice were bred continuously on a 129S6/SvEv genetic background. The urine samples were obtained from the mice at 6 weeks old. Protocols for use of experimental animals were approved by the Yale Institutional Animal Care and Use Committee. Animal handling and generation of slc26a6 null mice is detailed elsewhere.[4]

Chemicals

Sodium tetraborate decahydrate (STD), *β*-cyclodextrin sulfated (analytical grade, S*β*-CD) and methanol were purchased from Sigma-Aldrich (Steinheim, Germany), sodium dodecyl sulfate (SDS) and sodium hydroxide from Panreac Química S.A.U. (Barcelona, Spain), and hydrochloric acid from Fluka (Buchs, Switzerland). Reverse osmosed deionized water (Milli-Q Synthesis from Millipore, Bedford, MA, USA) was used for standard solution and electrolyte preparations. All the standards used for peak identification were obtained from Sigma Aldrich.

^{1}H NMR Sample Treatment and Instrument Conditions

Urine samples were prepared with pH 7.4 phosphate buffer as described previously.[8] ^{1}H NMR spectroscopy was performed at 300 K on a Bruker 800 MHz spectrometer (Bruker Biospin, Karlsruhe, Germany) using the following standard one-dimensional pulse sequence with saturation of the water resonance: Relaxation delay (RD)-90°-t_1-90°-t_m-90°-acquire free induction decay (FID), where 90° represents the applied 90° radio frequency (rf) pulse, t_1 is an interpulse delay set to a fixed interval of 3 ms, RD was 2 s and t_m (mixing time) was 100 ms. Water suppression was achieved through irradiation of the water signal during RD and t_m. Each urine spectrum was acquired using 8 dummy scans, 256 scans, 64 000 time domain points with a spectral width of 20 000 Hz. Prior to Fourier transformation, the FIDs were multiplied by an exponential function corresponding to a line broadening of 0.3 Hz.

CE-UV Sample Treatment and Instrumental Conditions

Metabolic fingerprinting was performed using two different separation modes:[9,10] a capillary zone electrophoresis method in reverse polarity (CZE-RP) that detects mainly anions, and a micellar electrokinetic chromatography method in normal polarity (MEKC-NP) that detects cations and neutral compounds.

CE experiments were carried out on a P/ACE MDQ system (Beckman Instruments, Fullerton, CA, USA) equipped with diode array UV-absorbance detection (190−600 nm), a temperature-controlled (liquid cooled) capillary compartment and an autosampler. Electrophoretic data were acquired and analyzed with 32 Karat software (P/ACE MDQ instrument).

Separations achieved with reverse polarity were performed using a capillary (Beckman Coulter, Buckinghamshire, England) coated with polyacrylamide (PAG) 60 cm in total length, 50 cm effective length and 50 μm internal diameter. On first use, the capillary was conditioned by a pressure flush of 0.1 M HCl (1 min), electrophoretic buffer (BGE1) (10 min) and an electrokinetic flush of electrolyte with 0.5 kV/cm (10 min). Between runs, the capillary was flushed under pressure with deionized water (2 min) and BGE1 (2 min). All experiments were performed at 25 °C using a separation potential of −20 kV. Samples were injected at the cathode, with 0.5 psi (3447 Pa) pressure applied for 10 s. The compounds were detected at the anode. BGE1 was prepared with 0.2 M phosphoric acid, adjusted to pH 6.10 with NaOH, and 10% (v/v) methanol added (the current observed under these conditions was 70 μA). Data were collected at a frequency of 4 Hz.

Separations achieved with normal polarity were performed in a fused silica capillary, 50 cm total, 40 cm effective length (50 μm internal diameter) (Composite Metal Services, Hallow, Worcester, U.K.). New capillaries were conditioned for 30 min at 25 °C with 1 M NaOH, followed by 0.1 M NaOH for 20 min and deionized water for 10 min. Before each analysis, the capillaries used were washed with 0.1 M HCl and deionized water for 1 min, and then 2 min with the run buffer. The running buffer (BGE2) comprised 25 mM sodium borate, 75 mM SDS and 6.25 mM sulfated *β*-cyclodextrin. The pH was adjusted to pH 9.50 with 1 M NaOH, after addition of SDS and cyclodextrin. Buffer solutions were filtered through a 45 μm filter before use. The capillary was maintained at 20 °C, with 18 kV applied voltage and 5 s hydrodynamic injection.

All the samples were initially run in CZE-RP method using an acidified urine sample. Afterwards, the same samples were mixed with 5 μL of BGE2 and 40 μL of water for MEKC-NP method.

Peak identification was the main drawback of CE-UV due to the selectivity of the UV detector. We were also limited by the small amount of sample. Peak assignment was performed by spiking the sample with standards and comparing migration times and spectral absorption.

Preprocessing and Data Analysis

^{1}H NMR Spectroscopy. The spectra were automatically phased, baseline corrected and referenced to 3-(trimethylsilyl)

dx.doi.org/10.1021/pr2012544 | J. Proteome Res. 2012, 11, 4425−4435

propionate-2,2,3,3-d_4 (TSP; δ 0.0) using an in-house routine written in MATLAB (The MathWorks, Natick, Massachusetts). Spectral regions corresponding to water and urea resonances (δ 4.5−6.5) were removed, and spectra were normalized using the probabilistic quotient method.[11]

The NMR peak assignments were based on published literature chemical shifts.[12,13] Chemical shifts belonging to the same metabolite were assigned by statistical total correlation spectroscopy (STOCSY) using an in-house Matlab script.[14]

CE-UV. Raw profiles from both polarities were treated with an in-house program developed in Matlab 7.0. First they were baseline corrected and aligned separately using the correlation optimized warping (COW) method previously described;[15] later both polarities were joined, first the signals from MEKC-NP mode followed by signals from CZE-RP profile. The maximum value for hippurate, a signal that appears in both profiles, was obtained, and the ratio between both hippurate signals was used for scaling. Subsequently all the data were normalized to the probabilistic quotient,[11] and the resultant matrix was submitted to multivariate data analysis with SIMCA P+ 12.0.

NMR-CE. Raw data from NMR and CE were combined in a single matrix after baseline correction, normalization and multialignment had been independently achieved. Both data sets were scaled to the highest peak in the profile to give equal weight to all signals.

Principal component analysis (PCA) was performed with the combined data set (^{1}H NMR, CE-UV and NMR-CE) in order to generate metabolic profiling data. Moreover, partial least square discriminant analysis (PLS-DA) and orthogonal partial least square discriminant analysis (OPLS-DA)[16] were also carried out to characterize the metabolic consequences of slc26a6 deletion in mice.

Every model was built using pareto scaling,[17] and the quality of the models was assessed by the cumulative R^2 value, and the predictive ability by cumulative Q^2 extracted according to the internal 7-fold cross-validation[18] default method of Umetrics SIMCA-P+12.0.1 software. The significance of the discriminatory metabolites was validated using a combination of cross validation and jackknife intervals.

Furthermore for NMR-CE, a program developed in Matlab based on the Pearson correlation coefficient, known as capillary electrophoresis−nuclear magnetic resonance statistical heteroanalytical correlation spectroscopy (CE−NMR-SHY), was applied in order to establish and plot single linear correlations among variables deriving from the two different techniques.[19] These correlations were driven from selected identified metabolite signals in the NMR or CE profiles that differentiated the slc26a6-null mice from the wild type. They were further analyzed to aid peak identification and to establish possible pathway associations with other metabolites. As in previous studies,[19] correlations greater than a threshold θ of 0.3 for this CE−NMR-SHY, corresponding to high sensitivity and a high probability of detecting structural correlations, were plotted.

RESULTS AND DISCUSSION

Metabolic Phenotyping of the slc26a6 Null Mouse Model

Clear metabolic differentiation was found between slc26a6 null mice and wild type control mice for both analytical techniques, namely NMR spectroscopy (Figure 1A,B) and CE-UV (Figure 2A,B). The CE-UV data presented are the result of the combination of two modes of CE separation in which the total profile contains cations, anions and neutral compounds.[20,21] A strong metabolic signature discriminating male and female mice was also apparent in both data sets. Several of the strain dependent metabolic differences were found to correlate with urinary oxalate.

Characterization of the Metabolic Phenotype of slc26a6 Null Mice Using ^{1}H NMR Spectroscopy. Significant changes were observed in the global ^{1}H NMR metabolic fingerprint of the SLC26A6-null mice urine, showing the strong impact of genetic modulation on the urine composition (Figure 1A,B). These differences manifest in the PCA scores plot as driving the variation in the second component (t2) (Figure 3A). The first component (t1) was dominated by variation relating to sex differences specifically: trimethylamine (TMA 2.88 (s)) and spermine (3.12 (m), 2.138 (m)) were higher in concentration in male mice and glycerate (4.09 (dd)), formate (8.46 (s)) and citrate (2.68 (d), 2.54 (d)) were higher in female mice. Regardless of sex differences, the slc26a6-null phenotype was dominated by higher urinary concentrations of (*m*-HPPS) (7.38 (t), 7.21 (m), 2.91 (t), 2.51 (t), 7.16 (dd)) and lower urinary hippurate signals (7.84 (d), 7.64 (t), 7.56 (t), 3.97 (d)) in comparison with the wild type mice (Figure 1D). The PCA model coefficients also indicated higher urinary levels of trimethylamine-*N*-oxide (TMAO) and creatine were associated with slc26a6 null mice with respect to the wild type mice.

OPLS-DA models were built to compensate for the effect of gender on the model in order to obtain a more direct profile of the slc26a6-related influence. In addition to the differential slc26a6 related metabolites identified from the PCA models, OPLS-DA also ranked scyllo-inositol, lactate and alanine as significantly higher in the urine of slc26a6 mice, whereas urinary excretion of hippurate, taurine and TMA was lower in the slc26a6 group.

Characterization of the Metabolic Phenotype of slc26a6 Null Mice Using CE-UV. The CE-UV derived metabolic phenotype of slc26a6 null mice was stronger than the NMR derived phenotype (Figure 2A,B), with separation of slc26a6 null and wild type control mice dominating the first component of the PCA model and sex differences influencing the second component (Figure 3B). Most metabolites were structurally identified, but some significantly discriminatory signals could not be assigned to known metabolites since the identity of metabolites from CE-UV analysis is reliant on comparison of migration time and spectral absorbance of the pure standard; this is only achieved by careful spiking of samples. As can be seen from Figure 2C, slc26a6 null mice showed higher levels of *m*-HPPS (Var_6718), oxalate (Var_5727) and allantoin (Var_2122). On the other hand, hippurate levels (Var_2220 in normal polarity and Var_9726 in reverse polarity) were consistently higher in wild type control mice.

The difference between the two analytical techniques in terms of the contribution of genetic background and gender to the overall variance sources of variance can be attributed to the differential capacity of each analytical technique to visualize different types of compounds within a biological sample. For example, oxalate and nitrate are observable in the CE-UV but not the ^{1}H NMR spectra, whereas taurine and the methylamines are more readily observable in the NMR profiles. However, both techniques contribute information on different metabolites to the total metabolic profile and together extend the coverage of the metabolome. Moreover, the metabolites that are detected by both techniques provide confirmation of the models, and thus the two analytical technologies are highly complementary.

The main discriminatory features of slc26a6 deletion in mice in the CE-UV PCA model were higher concentrations of *m*-HPPS and oxalate and lower concentrations of hippurate in comparison

dx.doi.org/10.1021/pr2012544 | J. Proteome Res. 2012, 11, 4425−4435

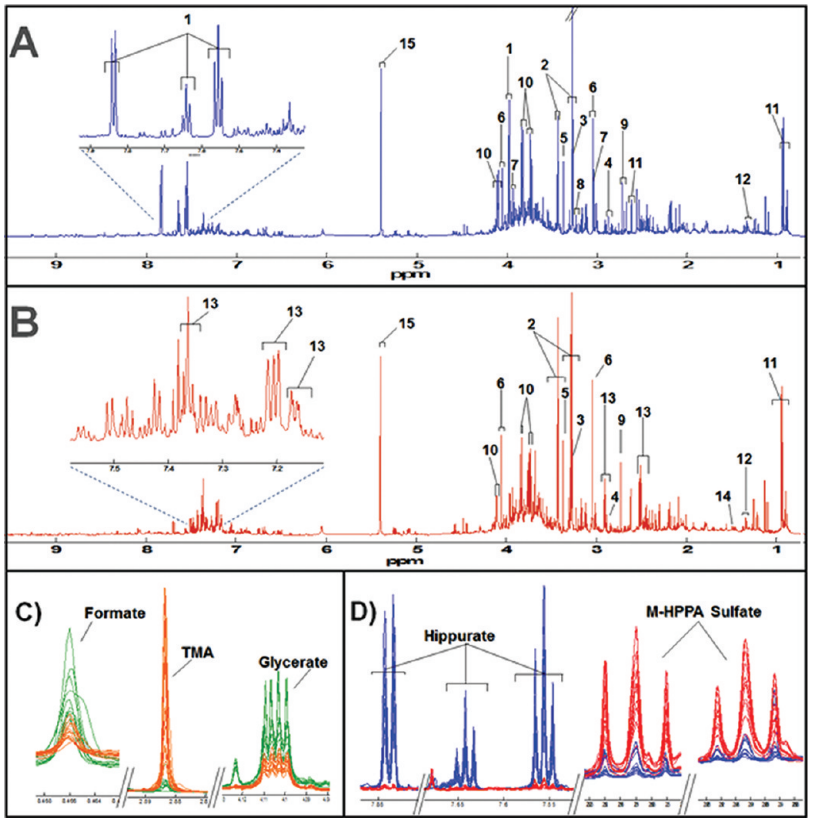

Figure 1. Typical 800 MHz ^{1}HNMR spectra of urine obtained from a male wild type mouse (A) and a male null-SLC26A6 mouse (B). Fragments of the NMR spectra (data aligned and normalized) showing differences in some of the discriminant metabolites according to the gender (C) and knockout condition (D). 1. Hippurate [δ 7.84 (d), 7.64 (t), 7.56 (t), 3.97 (d)]; 2. Taurine [δ 3.43 (t), 3.27 (t)]; 3. Trimthylamine *N*-oxide (TMAO) [δ 3.27 (s)]; 4. Trimethylamine (TMA) [δ 2.88 (s)]; 5. Scyllo inositol [δ 3.36 (s)]; 6. Creatinine [δ 4.05 (s), 3.045 (s)]; 7. Creatine [δ 3.93 (s), 3.04 (s)]; 8. Glycerophosphoryl choline [δ 3.23 (s)]; 9. Dimethylamine [δ 2.72 (s)]; 10. Glycerate [δ 4.09 (dd), 3.83 (dd), 3.72 (dd)]; 11. α-Ketoisocaproate [δ 2.62 (d), 0.94 (d)]; 12. Lactate [δ 4.11(q), 1.33 (d)]; 13. *m*-HPPA sulfate (*m*-HPPS) [δ 7.38 (t), 7.21 (m), 7.16 (dd), 2.91 (t), 2.51 (t)]; 14. Alanine [δ 3.79 (qt), 1.48 (d)].

with the wild type group. The OPLS-DA model was able to identify further discriminatory features including higher excretion of allantoin and chlorides, whereas citrate was positively associated with the wild type control.

Characterization of the Metabolic Phenotype of slc26a6 Null Mice Combining Two Analytical Platforms: ^{1}H NMR Spectroscopy and CE-UV. Statistical integration of nuclear magnetic resonance (NMR) spectroscopy and capillary electrophoresis (CE) data has been previously demonstrated in a mouse model based on urinary metabolite profiles[19] with a view to combining their different strengths and advantages, with regard to the ability to differentiate between different biological conditions and to identify potential metabolic pathways of response.

This data integration strategy was applied to the metabolic characterization of slc26a null mice compared to wild type control using a combination of high resolution ^{1}H NMR spectroscopy and CE with ultraviolet detection (UV) in order to achieve a more complete global metabolic profile in which oxalate is included.

PCA score plots derived from the combined data set (Figure 3C) showed grouping of samples according to gender along the first component (t1) as well as clear separation between wild type control and slc26a6 null mice along the second component (t2), indicating that the metabolic characteristics of the groups are markedly different. The combination of both analytical techniques allowed visualization of a broader range of metabolites in the same profile. Moreover, the enhanced quality of the model built using the combined data set over the PCA models generated from individual analytical methods can be measured by the increase in predictive capability of the models (Q^2), which increased from 0.34 (CE) and 0.39 (NMR) to 0.45 for the combined NMR-CE (Figure 3).

The OPLS-DA model, used as before to reduce the influence of gender on the model, found clear separation between the slc26a6 null and wild type groups along the predictive component on the OPLS-DA cross-validated scores plots (Figure 4A) of the NMR-CE combined data set. Variables with higher covariance on the predictive OPLS-DA component were identified from the S-plots. Higher levels of *m*-HPPS, oxalate, scyllo-inositol, TMAO, creatine, lactate, alanine, chlorides, allantoin and glycolate were characteristic of slc26a6 null mice, while higher urinary levels of hippurate, taurine, TMA, succinate, methionine, citrate were features of wild type mice. The significance of these metabolites as characteristic of the genetic strain was confirmed using the jack-knife interval (Figure 4B, Supporting Information Table S1). When the interval includes zero value, the covariance is not significant and the compound should not be considered as a potential biomarker. For this reason, creatinine, although apparently discriminatory in the OPLS-DA models was excluded from the Supporting Information Table S1, which summarizes the potential candidate biomarkers indicated by the plot and lists the discriminant metabolites obtained individually by each technique. Spearman rank correlation between variables intensity and

dx.doi.org/10.1021/pr2012544 | *J. Proteome Res.* 2012, 11, 4425–4435

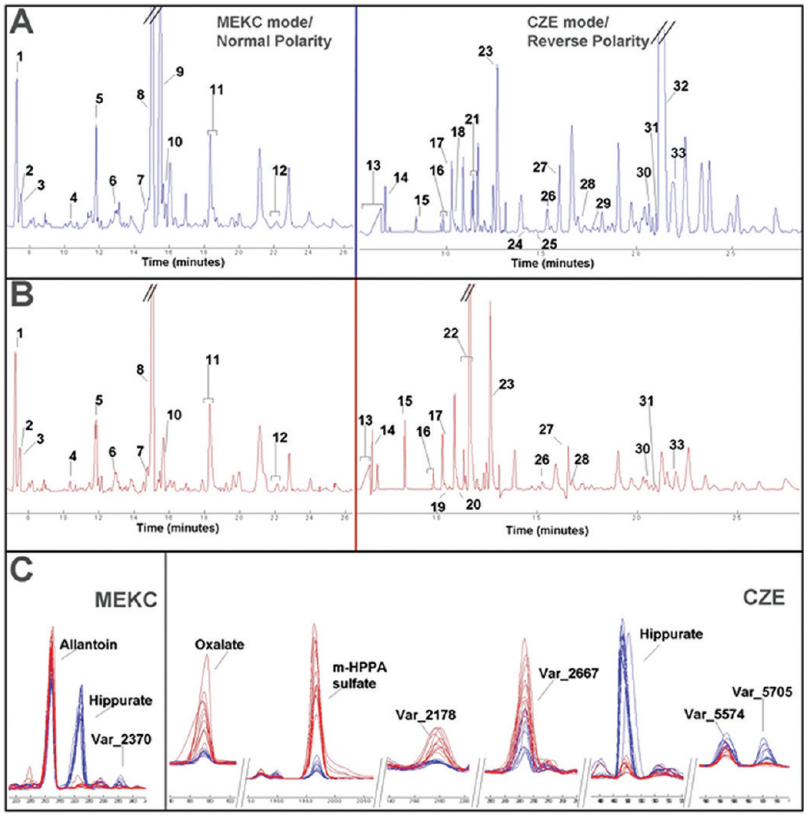

Figure 2. CE-UV metabolic fingerprinting of urine corresponding to male wild type mouse (A) and male SLC26A6-null mouse (B). Different levels observed in some metabolites according to the knockout condition (C). 1. Urea; 2. Creatinine; 3. Creatine; 4. Histidine; 5. Phenylalanine; 6. Methyluridine; 7. PAG; 8. Allantoin; 9. Hippurate; 10. Uridine; 11. Uric/Inosine; 12. Benzoate; 13. Chlorides; 14. Nitrate; 15. Oxalate; 16. Fumarate; 17. Oxoglutarate; 18. Succinate; 19. Isocitrate; 20. Glutarate; 21. Citrate; 22. *m*-HPPA sulfate (theorical); 23. Glycolate (coelutes); 24. Acetoacetate; 25. Lactate; 26. Ketosiovalerate; 27. Glycerate/Benzoate; 28. α-Ketoisocaproate; 29. Phenylpyruvate; 30. Phenyllactate; 31. Glutamate; 32. Hippurate/Vanillate 33. Ascorbate. Wild type control highlighted in blue. SLC26A6-null mice highlighted in red.

group for metabolites found to be significant using OPLSDA and jack-knifing is also provided in Supporting Information Table S1. The discrete distribution of the classes, slc26a6 null ($n = 11$) and wild type ($n = 8$), also causes a discrete distribution in the rank correlation. In this study, the highest absolute rank correlation (fully separated groups) that can be achieved is 0.856 with a corresponding p-value of 2.89×10^{-6}, because of the discrete group levels indicating a true and marked difference in the metabolism of the SLC26A6 null mice. Finally, using the p-values determined with the Spearman correlation, we have calculated the corresponding q-values using the false discovery rate[22] (FDR) using the R-package fdrtool.[23] We chose to allow 5% false discoveries ($q \leq 0.05$) for our findings. The metabolites that remain positively associated with slc26a6 deletion, after FDR, are *m*-HPPA, lactate, glycerolphosphorylcholine and oxalate. Hippurate remains negatively associated with slc26a6 deletion.

Influence of Gender on the Metabolic Phenotype of slc26a6 Null Mice. On the basis of the results obtained from the PCA model, OPLS-DA models were performed in order to study the influence of gender and to determine if the metabolic features of slc26a6 mice were consistent for male and female animals. Clear clustering in both the PCA and the OPLS-DA scores plots due to gender was also observed. Discriminant metabolites for female mice were identified by NMR and CE separately. Higher urinary concentrations of TMAO, creatine, 2-oxoisocaproate, 3-methyl-2-oxovalerate, *m*-HPPS, citrate and glycerate were associated with female mice in the NMR profiles. Conversely, TMA, methionine, spermine and alanine were positively associated with male mice. Further gender dimorphic metabolites extracted from the more OPLS-DA models of the CE-UV data were uridine (higher in females) and urea, penylalanine and allantoin (higher in males). As before, the statistical significance of the metabolites was confirmed by jack-knife interval (Figure 5A,B).

Supporting Information Table S2 shows the Spearman rank correlation (RHO correlation) between male ($n = 11$) and female ($n = 8$) mice. These result in the same discrete possible rank correlations as in the slc26a6 null versus wild type comparison in Supporting Information Table S1. Of the metabolites manifesting sex differences in urinary concentration in the current experiment, guanidinoacetate, creatine, creatinine, spermine, TMA and trimethylamine-*N*-oxide (TMAO) have previously been reported in mice.[1] Sex differences for urinary creatine and citrate concentrations have also previously been reported for humans with higher excretion in females,[2] consistent with the observations in the current study. Guanidinoacetate, also excreted in higher concentrations in female urine, is converted into creatine in the liver using *S*-adenosylmethionine as the methyl donor,[3] and therefore it is possible that this pathway is up-regulated in females.

Higher levels of TMAO have been reported in female Han Wistar rats than in male rats.[24] Hippurate, succinate, 2-oxoglutarate and dimethylglycine were elevated in the urine of females.[25] Of the metabolites strongly correlated with gender, creatine, uric acid, trimethylamine, methionine, alanine and TMAO were also correlated with the slc26a6 null group and thus deconvolution of the gender versus slc26a6 transporter deletion effects is complicated.

dx.doi.org/10.1021/pr2012544 | *J. Proteome Res.* 2012, 11, 4425–4435

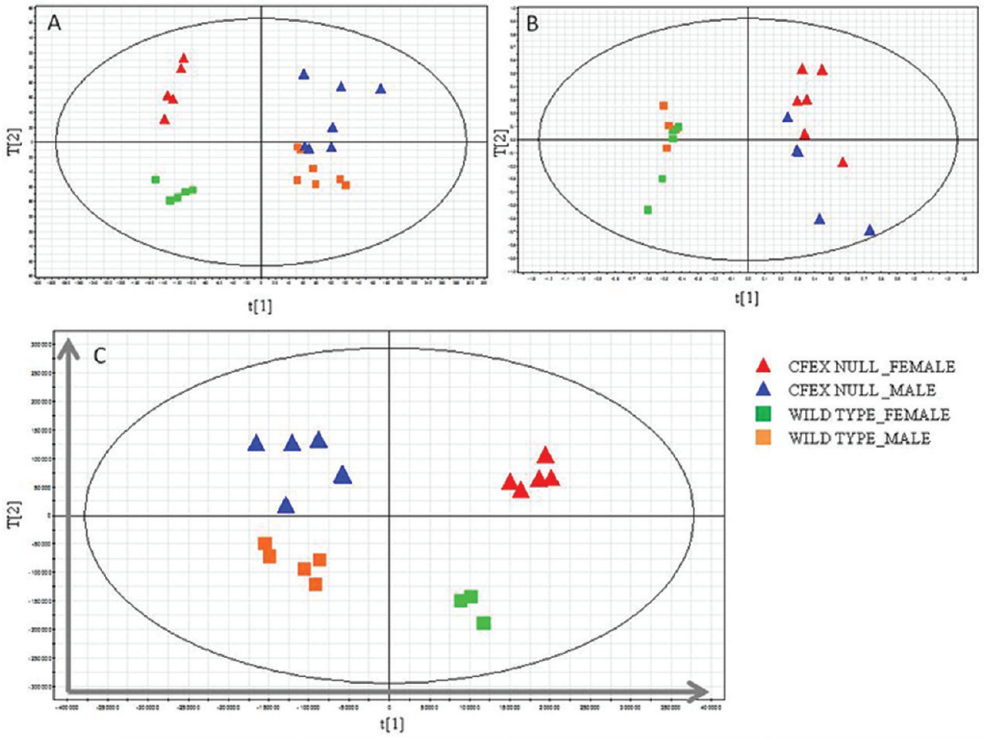

PCA	NMR		CE		NMR-CE	
	R^2X(cum)	Q^2(cum)	R^2X(cum)	Q^2(cum)	R^2X(cum)	Q^2(cum)
1 Component	0.50	0.30	0.32	0.24	0.35	0.25
[1+2] Component	0.62	0.34	0.49	0.33	0.56	0.43
[1+2+3] Component	0.69	0.39	0.57	0.34	0.64	0.45

Figure 3. Scores plots from the PCA model derived from the NMR (A), CE (B), and NMR_CE combined data set (C) using pareto scaling (red triangle, knockout female; blue triangle, knockout male; green box, wild type female; orange box, wild type male).

Although the main source of TMA is the bacterial breakdown of choline in the intestine, this metabolite may have a wider role in physiology and may act as a signaling molecule. Methylamines, particularly TMA, have been shown to be present in higher concentrations in the urine of male mice and are lower in castrated mice.[26,27] Trace amine-associated receptors are thought to act as pheromone receptors in the nose,[28] a hypothesis that is supported by the fact that several of these trace amines such as TMA and isoamylamine can speed up puberty in female mice. Conversely, urinary concentrations of TMAO are higher in female mice. TMAO can be generated from the oxidation of TMA via hepatic flavin monooxygenase enzymes, predominantly FMO3,[27] which is derived from dietary constituents such as choline. However TMAO can also be directly absorbed from food. For example, cold water dwelling fish typically contain high levels of this metabolite, as it has antifreeze functions.

m-HPPS excretion has been shown both in the current study and previous studies to be influenced by gender. In the present study, it is also highly correlated with the slc26a6-null group. Stanley et al. reported higher concentrations of *m*-HPPS sulfate in male rat urine samples, which reflects the higher sulfation activity of male sulfotransferase enzymes in rats.[30] Sex differences in sulfation are well documented with four times higher cytosolic sulfation in male rat liver compared with females. However, this sex-related difference was reversed in mice, with female mice showing the higher sulfating activity, which fits with the higher levels of HPPS observed in female mice in the current study.[31]

As for the slc26a6 deletion findings, we have calculated the corresponding *q*-values using FDR with respect to sex differences. For the gender comparison TMA, alanine, PAG and spermine remain positively associated with male mice after exclusion based on *q*-values. *m*-HPPA, formate, TMAO, creatine, creatinine, 2-oxoisocaproate, 3-methyl-2-oxoisovalerate, glycerate, guanidinoacetate and methylmalonate remain positively associated with female mice.[29]

Identification of Statistical Correlation between the Two Main Phenotypic Characteristics, Oxalate and *m*-HPPS with the Global Urine Profiles

Bidirectional correlation analysis of the combined data set (NMR-CE) was applied in order to establish pairwise correlations structures. It was also used for metabolic or functional correlations either within or between NMR and CE data,[19] such as those between molecules related by pathway or shared response to the slc26a6 deletion.

Since oxalate (Var_5727, *p*-value <0.05), a molecule that can be exchanged by slc26a6 and plays a key role in the characterization of slc26a6 deletion, is NMR invisible, a correlation matrix was calculated for the combined CE-UV and NMR detected signals using the oxalate signal in the CE-UV trace as the driver. A univariate Pearson correlation matrix encompassing all NMR and CE data was used with the oxalate signal with a cutoff level of $p < 0.05$. Signals that covaried across the NMR-CE data set are colored in red (Figure 6) and indicate a significant correlation ($p < 0.05$) with the oxalate signal. These signals included *m*-HPPS (signals on NMR; triplet δ 7.38 (r) 0.497, multiplet δ 7.21 (r) 0.559, triplet δ 2.91 (r) 0.561, triplet

dx.doi.org/10.1021/pr2012544 | *J. Proteome Res.* 2012, 11, 4425–4435

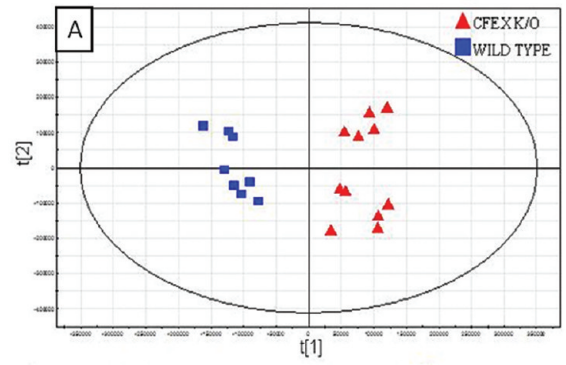

OPLSDA	NMR-CE CFEX KO vs WILD TYPE		
	R^2X (cum)	R^2Y (cum)	Q^2(cum)
1 Component	0.23	0.55	0.62
[1+2] Component	0.91	0.94	0.98

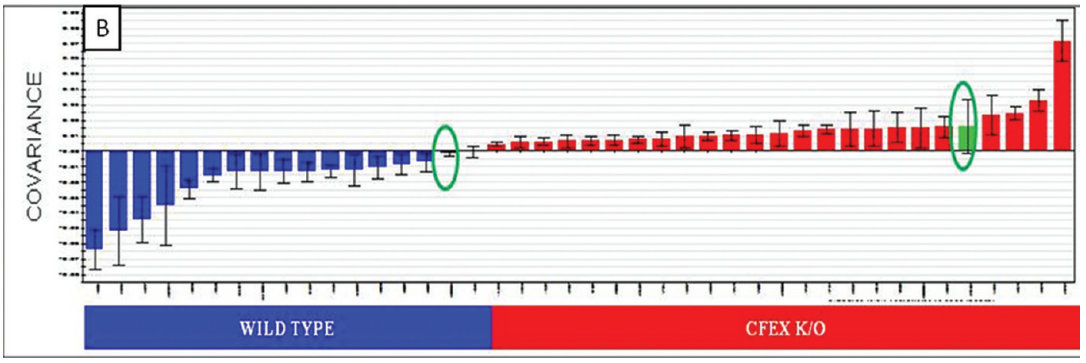

Figure 4. (A) Scores plot from OPLS-DA model derived from the NMR_CE data showing separation according to slc26a6-null and wild type mice. (B) Covariance for discriminant variables in the wild type and slc26a6-null mice including jack-knife interval (p > 95%); green bars show no statistical significance as determined by the interval which includes zero value.

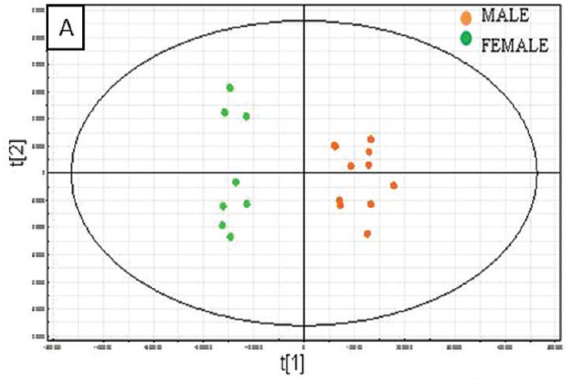

OPLSDA	NMR-CE _ FEMALE VS MALE		
	R^2X (cum)	R^2Y (cum)	Q^2(cum)
1 Component	0.35	0.95	0.91
[1+2] Component	0.45	0.98	0.95

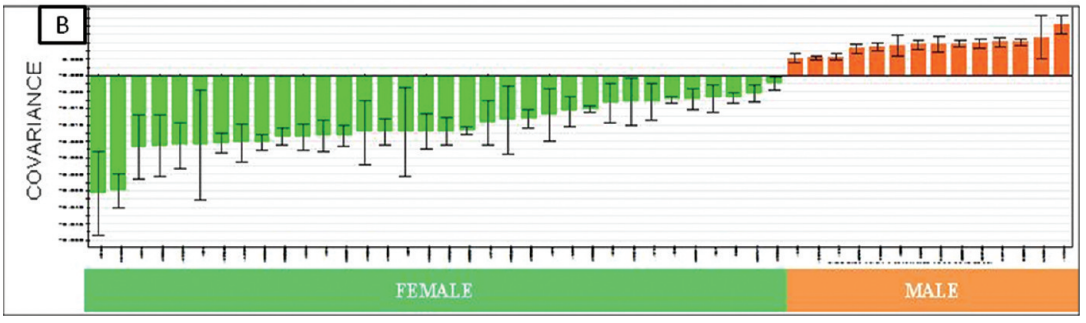

Figure 5. (A) Scores plot from the OPLS-DA model derived from the NMR_CE data showing separation according to gender (B) Covariance for discriminant variables in female and male mice including jack-knife interval (p > 95%).

δ 2.51 (r) 0.563, doublets of doublets δ 7.16 (r) 6.00, and in CE; Var_6718 (r) 0.886), TMAO (singlet δ 3.27 (r) 0.600), lactate (doublet δ1.33 (r) 0.610), chlorides (Var_5164 (r) 0.549), nitrate (Var_5228 (r) 0.718), fumarate (Var_6168 0.580), 2-oxoglutarate

dx.doi.org/10.1021/pr2012544 | J. Proteome Res. 2012, 11, 4425–4435

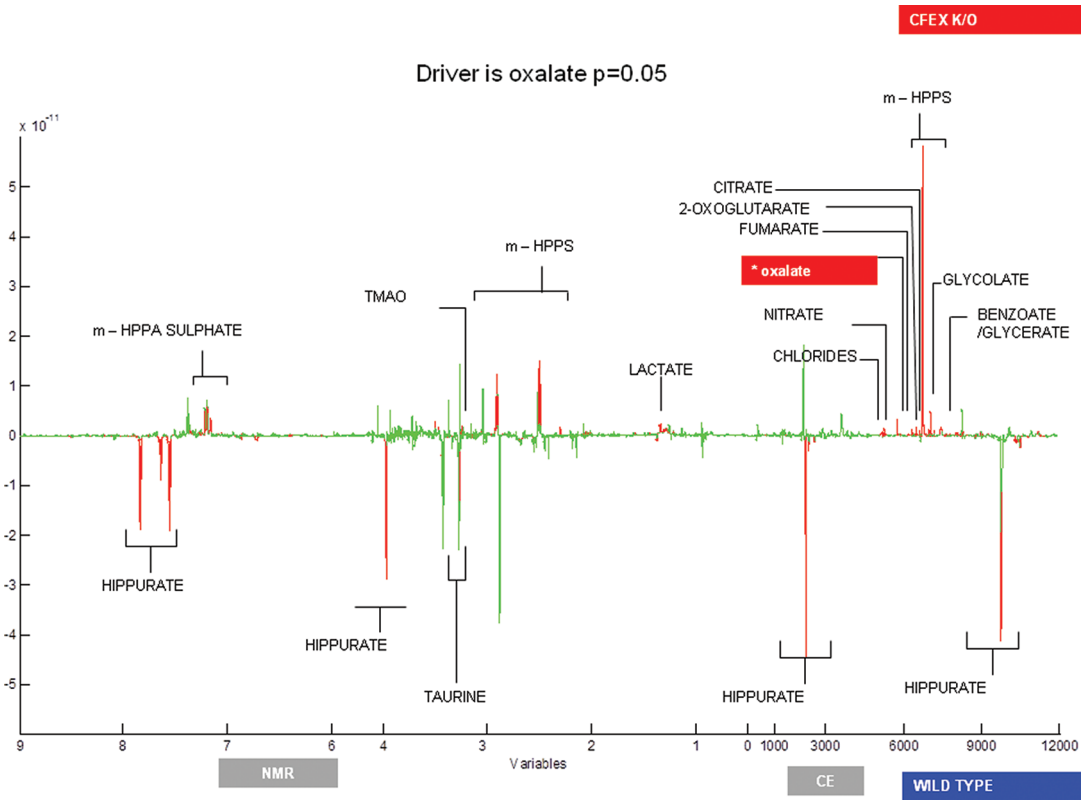

Figure 6. Correlation structure obtained after selecting oxalate in CE and applying a $p = 0.05$ significance criterion. Signals positively and highly correlated to oxalate signal can be seen highlighted in red on the top hemisphere of the figure, such as *m*-HPPS [signals on NMR; triplet δ 7.38 (r) 0.497, multiplet δ 7.21 (r) 0.559, triplet δ 2.91 (r) 0.561, triplet δ 2.51 (r) 0.563, doublets of doublets δ 7.16 (r) 6.00, and on CE; Var_6718 (r) 0.886], TMAO [singlet δ 3.27 (r) 0.600], lactate [doublet δ1.33 (r) 0.610], chlorides [Var_5164 (r) 0.549], nitrate [Var_5228 (r) 0.718], fumarate [Var_6168 0.580], 2-oxoglutarate [Var_6308 (r) 0.619], glutamate [Var_6528 (r) 0.730], citrate [Var_6628 (r) 0.757], glycolate [Var_7038 (r) 0.825], benzoate/glycerate [Var_8968 (r) 0.640]. Signals highly but negatively correlated to oxalate signal can be seen at the bottom hemisphere of the figure, also highlighted in red, hippurate [signals on NMR; doublet δ 7.84 (r) −0.599, triplet δ 7.64 (r) −0.595, triplet δ 7.56 (r) −0.596, doublet δ 3.97 (r) −0.600, and on CE; Var_2220 (r) −0.761, Var_9726 (r) −0.701], taurine [triplet δ 3.43 (r) −0.490, triplet δ 3.27 (r) −0.516].

(Var_6308 (r) 0.619), glutamate (Var_6528 (r) 0.730), citrate (Var_6628 (r) 0.757), glycolate (Var_7038 (r) 0.825), benzoate/glycerate (Var_8968 (r) 0.640), which also revealed positive correlation with oxalate. Moreover, hippurate (signals on NMR; doublet δ 7.84 (r) −0.599, triplet δ 7.64 (r) −0.595, triplet δ 7.56 (r) −0.596, doublet δ 3.97 (r) −0.600, and on CE; Var_2220 (r) −0.761, Var_9726 (r) −0.701), and taurine (triplet δ 3.43 (r) −0.490, triplet δ 3.27 (r) −0.516) were significantly anticorrelated with oxalate (Figure 6); *p*-values and correlation coefficients, corresponding to the signals for metabolites that statistically correlate with oxalate, can be seen in Supporting Information Table S3.

The general assumption would be that metabolites that are strongly significantly correlated are more likely to be related to each other either mechanistically, e.g., in a shared perturbed metabolic pathway, or undergoing a similar metabolic response to the genetic modification. Thus oxalate was most strongly associated with *m*-HPPS, glycolate, citrate, nitrate (all positive) and hippurate (negative). The association between oxalate and nitrate simply reflects the capacity of the transporter for carrying multiple anions.[8] Chloride was positively correlated to oxalate, but as it was added to every sample in order to ensure the complete oxalate solubility in the urine, its biological significance was not considered in the correlations. Glycolate is one of the precursors for oxalate, together with glycine, hydroxyproline and glyoxalate;[9] the other precursors were not indicated as discriminatory of the slc26a6 null model, nor were they significantly correlated with oxalate.

One of the strongest metabolic correlations with oxalate, and indeed one of the strongest metabolites characterizing the metabolic phenotype of the slc26a6 mouse, was *m*-HPPS. The correlation matrix driven from *m*-HPPS showed correlations with hippurate (negative) creatinine, methylmalonate, creatine and TMAO (positive). Here the picture is confounded slightly since *m*-HPPS, although highly discriminatory for the slc26a6-null class, is also consistently higher in female mice over males. Thus, some of the metabolites that were correlated to *m*-HPPS, such as creatinine and TMA, may be reflective of sex-related differences in metabolism rather than the genetic modification.

m-HPPS was found to be strongly discriminant for slc26a6 deletion in both the combined and gender stratified models, but was also modestly discriminant for gender. Since this metabolite was one of the most influential in characterizing the slc26a6 phenotype, a correlation network was also calculated in order to explore potential pathway connections.

A correlation matrix was calculated for the triplet δ 2.91, *p*-value = 1.93×10^{-5} of *m*-HPPS, as this was the signal with the highest significance in discriminating the slc26a6 null group and that also occurs in a spectral region with minimal spectral overlap from other metabolite resonances. As can be seen in Figure 7, TMAO (singlet δ 3.27 (r) 0.629), creatine (singlet δ 3.04 (r)

dx.doi.org/10.1021/pr2012544 | J. Proteome Res. 2012, 11, 4425–4435

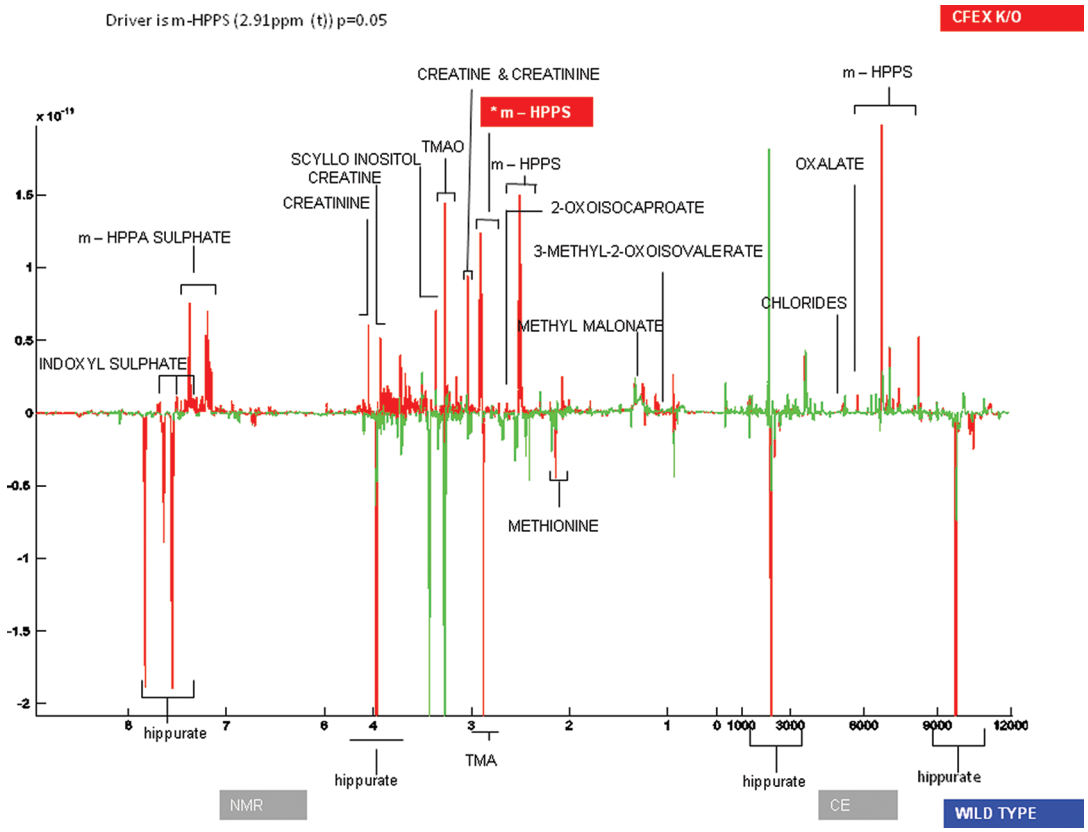

Figure 7. Correlation structure obtained after selecting *m*-HPPS on NMR and applying a $p = 0.05$ significance criterion. Signals positively and highly correlated to oxalate signal can be seen highlighted in red on the top hemisphere of the figure, such as TMAO [singlet δ 3.27 (r) 0.629], creatine [singlet δ 3.04 (r) 0.687, singlet δ 3.93 (r) 0.573], creatinine [singlet δ 3.045 (r) 0.738, singlet δ 4.05 (r) 0.753], scyllo-inositol [singlet δ 3.37 (r) 0.492], α-ketoisocaproate [doublet δ 0.94 (r) 0.535, doublet δ 2.62 (r) 0.655], methyl malonate [doublet δ 1.25 (r) 0.734], α-keto-β-methyl-*N*-valerate [doublet δ 1.11 (r) 0.573], indoxylsulfate [doublet δ 7.71 (r) 0.661, doublet δ 7.50 (r) 0.673, singlet δ 7.36 (r) 0.576], chlorides [Var_5164 (r) 0.178] and oxalate [Var_5727 (r) 0.483]. Signals highly but negatively correlated to oxalate signal, such as hippurate [signals on NMR; doublet δ 7.84 (r) −0.693, triplet δ 7.64 (r) −0.669, triplet δ 7.56 (r) −0.666, doublet δ 3.97 (r) −0.592, and on CE; Var_2220 (r) −0.739, Var_9726 (r) −0.760], TMA [singlet δ 2.88 (r) −0.642] and methionine [singlet δ2.14 (r) −0.564], can be seen at the bottom hemisphere of the figure, also highlighted in red.

0.687, singlet δ 3.93 (r) 0.573), creatinine (singlet δ 3.045 (r) 0.738, singlet δ 4.05 (r) 0.753), scyllo-inositol (singlet δ 3.37 (r) 0.492), 2-oxoisocaproate (doublet δ 0.94 (r) 0.535, doublet δ 2.62 (r) 0.655), methyl malonate (doublet δ 1.25 (r) 0.734), 3-methyl-2-oxovalerate (doublet δ 1.11 (r) 0.573), indoxylsulfate (doublet δ 7.71 (r) 0.661, doublet δ 7.50 (r) 0.673, singlet δ 7.36 (r) 0.576), chlorides (Var_5164 (r) 0.178) and oxalate (Var_5727 (r) 0.483), were positively and highly correlated to *m*-HPPS signal. In the same way, signals corresponding to hippurate (signals on NMR; doublet δ 7.84 (r) −0.693, triplet δ 7.64 (r) −0.669, triplet δ 7.56 (r) −0.666, doublet δ 3.97 (r) −0.592, and on CE; Var_2220 (r) −0.739, Var_9726 (r) −0.760), TMA (singlet δ 2.88 (r) −0.642) and methionine (singlet δ 2.14 (r) −0.564), were strongly negatively correlated to *m*-HPPS. Supporting Information Table S4 shows *p*-values and correlation coefficients of these metabolites.

The use of correlation matrices can provide additional information to that extracted from the multivariate models. For example, nitrate falls below the significance level set for the multivariate models generated for the CE-UV data but is highlighted as a correlate of oxalate using the Pearson correlation statistic. Likewise the correlation matrix calculated for *m*-HPPS identifies indoxylsulfate and several other gut microbial metabolites (TMA, TMAO, hippurate and other phenolics) as strong correlates, thereby further supporting the metabolic signature of gut microbial metabolites, although indoxyl sulfate is not in itself identified as a discriminatory feature of the OPLS-DA models.

Differential Expression of Gut Microbial Metabolites in the slc26a6 Null Mouse

The use of transgenic models of altered intestinal transport can also probe the interactions between dietary substrates and the gut microbiota. There is increasing interest in the gut microbiome and the symbiotic relationship with its host, more specifically the influence it may have on host immunity and metabolism.[13] However, an aspect that has not been considered yet in any detail is whether alterations in intestinal nutrient transport can in turn affect metabolism by changing the gut microbes or their metabolism. Intestinal bacteria have their own metabolic pathways and metabolites, which may integrate with those of the host.[13]

Although the slc26a6 urine model was created to explore the relationship between renal anion exchange and sodium regulation, it is known that this anion exchange transporter is ubiquitously found throughout the intestine and other tissues, such as heart, kidney, and liver.[3] The strong differences in *m*-HPPS and hippurate suggest that the metabolic phenotype of this knockout is related at least partially to altered intestinal microbial presence or activity, which may be more closely associated with effects arising from the expression of this transporter in the intestine. *m*-HPPS is a metabolite product from the metabolism of caffeic acid (CA), ferulic acid (FA) and chlorogenic acid,

dx.doi.org/10.1021/pr2012544 | J. Proteome Res. 2012, 11, 4425−4435

which appears to occur in the intestinal mucosa and colonic microflora.[4] However, the major pathway forming *m*-HPPA is the reduction of caffeic acid to 3,4-dihydroxyphenylpropionic acid followed by dehydroxylation to *m*-HPPS by the action of the gut flora. Aromatic amino acids, including tyrosine, tryptophan and phenylalanine, are also dietary precursors of phenolic acid-related metabolites. The metabolic end points of the intestinal metabolism of tyrosine include phenylpropionic acid and *m*-HPPS.[10] The rate of excretion of *m*- and *p*-hydroxyphenyl-proionic acid has been shown to be low in germ free animals, since most of the *m*-hydroxyphenylproionic acid involves reduction of caffeic acid followed by para-dehydroxylation, which does not occur in germ free rats. *m*-HPPA excretion increases dramatically (~140 fold) upon inoculation with fecal micro-organisms,[11] which further supports the microbial origin of this metabolite.

Although the urinary concentrations of hippurate and *m*-HPPS do not appear to be stoichometrically related, other than oxalate levels, they represent the two most discriminatory metabolites for the slc26a6 null model and are anticorrelated. Hippurate is formed from the metabolism of dietary aromatic compounds to benzoate by the gut microbiota and subsequent conjugation of benzoate with glycine in the mitochondria. The concentration of urinary hippurate has been shown to be modulated according the composition of the intestinal microbiota,[15] and rats have been shown to switch from excreting hippurate as the predominant microbial metabolite to *m*-HPPA and vice versa in as little as a few hours.[32]

As mentioned previously, a Pearson correlation calculated for a selected *m*-HPPS signal identified a range of microbial metabolites or microbial−mammalian cometabolites including indoxylsulfate, TMA, TMAO, and hippurate.

The significance of urinary TMA and TMAO has been discussed in relation to sex differences. Altered urinary excretion of TMAO has been observed in previous studies, most commonly in cases of drug-induced nephrotoxicity,[5] but this metabolite has also been positively associated with cardiovascular disease in both humans and mouse models.[33] Feeding of hyperlipidemic mice with either choline or TMAO was shown to result in higher plasma levels of TMAO, which was directly associated with the size of atherosclerotic plaque. Higher plasma TMAO concentrations were found in female mice, which also developed more severe atherosclerosis than male mice.[33]

Another indication of potential gut microbial involvement with oxalate excretion is that intestinal colonization with the bacterium Oxalobacter formigenes, a normal gut commensal, appears to promote intestinal oxalate secretion and reduce urinary oxalate excretion in rats and mice.[12,30] Thus, although the role of the gut microbiota in defining the slc26a6 null mouse model is far from clear, the results point to the fact that microbial metabolites are differentially expressed in this model of anion transport. Taken together with the literature on choline metabolism, there may be a link with the hypertension associated with renal stone formation, but more detailed laboratory experiments using labeled substrates would be required to probe this link further.

CONCLUSIONS

In summary, we have found a strong metabolic phenotype for slc26a6 deletion, which is defined both by altered urinary composition of anions such as oxalate, chloride and nitrates and also by modified urinary metabolites deriving from gut microbial metabolism including *m*-HPPS, hippurate and methylamines. Differential levels of tricarboxylic acid cycle intermediates were also contributory to the metabolic signature of the slc26a6 null mice. The modification of the microbial metabolites is consistent with the fact that the slc26a6 transporter is found in a range of tissues other than the kidney, including the intestine. Sex-related differences were also found in the metabolic phenotype of slc26a6 null mice, which may relate to sex differences in renal stone formation and further may have implications in hypertension.

ASSOCIATED CONTENT

Supporting Information

Table S1: Metabolites observed in significantly different concentrations in urine samples obtained from slc26a6 null mice compared with wild-type control mice. Table S2: The changes of metabolites observed in urine obtained from female mice compared with male mice. Table S3: Summary of the metabolites that are positively and negatively associated with Oxalate (variable 5727), based on Pearson correlation. Table S4: Summary of the metabolites that are positively and negatively associated with *m*-HPPS (2.51 (t) ppm), based on Pearson correlation. This material is available free of charge via the Internet at http://pubs.acs.org.

AUTHOR INFORMATION

Corresponding Author

*Tel.: +44 (0) 20 7594 3220. Fax: +44 (0) 20 7594 3226. E-mail: elaine.holmes@imperial.ac.uk.

Author Contributions

⊥These authors contributed equally.

Notes

The authors declare no competing financial interest.

ACKNOWLEDGMENTS

The INTERMAP Study has been supported by Grants R01-HL050490 and R01-HL084228 from the National Heart, Lung, and Blood Institute, National Institutes of Health, Bethesda, Maryland, USA and by the Chicago Health Research Foundation. CEMBIO authors acknowledge EADS-CASA. Alma Villaseñor thanks Santander Bank for the mobility grant. Paul Elliott acknowledges funding support from the National Institute for Health Research (NIHR) Biomedical Research Centre, Imperial College Healthcare NHS Trust. He is an NIHR senior investigator.

REFERENCES

(1) Worcester, E. M.; Coe, F. L. Nephrolithiasis. *Primary Care* **2008**, *35* (2), 369−91.

(2) Johri, N.; Cooper, B.; Robertson, W.; Choong, S.; Rickards, D.; Unwin, R. An update and practical guide to renal stone management. *Nephron Clin. Pract.* **2010**, *116* (3), c159−71.

(3) Aronson, P. Essential roles of CFEX-mediated Cl(-)-oxalate exchange in proximal tubule NaCl transport and prevention of urolithiasis. *Kidney Int.* **2006**, *70* (7), 1207−13.

(4) Jiang, Z.; Asplin, J.; Evan, A.; Rajendran, V.; Velazquez, H.; Nottoli, T.; Binder, H.; Aronson, P. Calcium oxalate urolithiasis in mice lacking anion transporter Slc26a6. *Nat. Genet.* **2006**, *38* (4), 474−8.

(5) Holmes, E.; Loo, R. L.; Stamler, J.; Bictash, M.; Yap, I. K.; Chan, Q.; Ebbels, T.; De Iorio, M.; Brown, I. J.; Veselkov, K. A.; Daviglus, M. L.; Kesteloot, H.; Ueshima, H.; Zhao, L.; Nicholson, J. K.; Elliott, P. Human metabolic phenotype diversity and its association with diet and blood pressure. *Nature* **2008**, *453* (7193), 396−400.

(6) Parmar, M. S. Kidney stones. *BMJ [Br. Med. J.]* **2004**, *328* (7453), 1420−4.

(7) Aronson, P. Role of anion transporter SLC26A6 (CFEX) in prevention of hyperoxaluria and urolithiasis. *AIP Conf. Proc.* **2007**, *900* (1), 141−8.

(8) Beckonert, O.; Keun, H. C.; Ebbels, T. M.; Bundy, J.; Holmes, E.; Lindon, J. C.; Nicholson, J. K. Metabolic profiling, metabolomic and metabonomic procedures for NMR spectroscopy of urine, plasma, serum and tissue extracts. *Nat. Protoc.* **2007**, *2* (11), 2692−703.
(9) García, A.; Barbas, C.; Aguilar, R.; Castro, M. Capillary electrophoresis for rapid profiling of organic acidurias. *Clin. Chem.* **1998**, *44* (9), 1905−11.
(10) Vallejo, M.; Angulo, S.; García-Martínez, D.; García, A.; Barbas, C. New perspective of diabetes response to an antioxidant treatment through metabolic fingerprinting of urine by capillary electrophoresis. *J. Chromatogr., A* **2008**, *1187* (1−2), 267−74.
(11) Dieterle, F.; Ross, A.; Schlotterbeck, G.; Senn, H. Probabilistic quotient normalization as robust method to account for dilution of complex biological mixtures. Application in 1H NMR metabonomics. *Anal. Chem.* **2006**, *78* (13), 4281−90.
(12) Lindon, J.; Nicholson, J.; Everett, J. NMR Spectroscopy of biofluids. *Annu. Rep. NMR Spectrosc.* **1999**, *38*, 1−88.
(13) Martin, F. P.; Dumas, M. E.; Wang, Y.; Legido-Quigley, C.; Yap, I. K.; Tang, H.; Zirah, S.; Murphy, G. M.; Cloarec, O.; Lindon, J. C.; Sprenger, N.; Fay, L. B.; Kochhar, S.; van Bladeren, P.; Holmes, E.; Nicholson, J. K. A top-down systems biology view of microbiome-mammalian metabolic interactions in a mouse model. *Mol. Syst. Biol.* **2007**, *3*, 112.
(14) Cloarec, O.; Dumas, M. E.; Craig, A.; Barton, R. H.; Trygg, J.; Hudson, J.; Blancher, C.; Gauguier, D.; Lindon, J. C.; Holmes, E.; Nicholson, J. Statistical total correlation spectroscopy: an exploratory approach for latent biomarker identification from metabolic 1H NMR data sets. *Anal. Chem.* **2005**, *77* (5), 1282−9.
(15) Tomasi, G.; van den Bergand, F.; Andersson, C. Correlation optimized warping and dynamic time warping as preprocessing methods for chromatographic data. *J. Chemom.* **2004**, *18*, 231−241.
(16) Bylesjö, M.; Rantalainen, M.; Cloarec, O.; Nicholson, J.; Holmes, E.; Trygg, J. OPLS discriminant analysis: combining the strengths of PLS-DA and SIMCA classification. *J. Chemom.* **2006**, *20*, 341−351.
(17) van den Berg, R. A.; Hoefsloot, H. C.; Westerhuis, J. A.; Smilde, A. K.; van der Werf, M. J. Centering, scaling, and transformations: improving the biological information content of metabolomics data. *BMC Genomics* **2006**, *7*, 142.
(18) Eriksson, I.; Johansson, E.; Kettaneh-Wold, N.; Wold, S. *Multi- and Megavariate Data Analysis and Applications*; Umetrics: Umeå, Sweden, 2001; p 533.
(19) Garcia-Perez, I.; Couto Alves, A.; Angulo, S.; Li, J.; Utzinger, J.; Ebbels, T.; Legido-Quigley, C.; Nicholson, J.; Holmes, E.; Barbas, C. Bidirectional correlation of NMR and capillary electrophoresis fingerprints: a new approach to investigating *Schistosoma mansoni* infection in a mouse model. *Anal. Chem.* **2010**, *82* (1), 203−10.
(20) García-Pérez, I.; Whitfield, P.; Bartlett, A.; Angulo, S.; Legido-Quigley, C.; Hanna-Brown, M.; Barbas, C. Metabolic fingerprinting of *Schistosoma mansoni* infection in mice urine with capillary electrophoresis. *Electrophoresis* **2008**, *29* (15), 3201−6.
(21) Barbas, C.; Vallejo, M.; García, A.; Barlow, D.; Hanna-Brown, M. Capillary electrophoresis as a metabolomic tool in antioxidant therapy studies. *J. Pharm. Biomed. Anal.* **2008**, *47* (2), 388−98.
(22) Benjamini, Y.; Hochberg, Y. Controlling the false discovery rate: a practical and powerful approach to multiple testing. *J. R. Stat. Soc., Ser. B* **1995**, *57* (1), 12.
(23) Strimmer, K. fdrtool: a versatile R package for estimating local and tail area-based false discovery rates. *Bioinformatics* **2008**, *24* (12), 1461−2.
(24) Stanley, E. G.; Bailey, N. J.; Bollard, M. E.; Haselden, J. N.; Waterfield, C. J.; Holmes, E.; Nicholson, J. K. Sexual dimorphism in urinary metabolite profiles of Han Wistar rats revealed by nuclear-magnetic-resonance-based metabonomics. *Anal. Biochem.* **2005**, *343* (2), 195−202.
(25) Williams, R. E.; Lenz, E. M.; Lowden, J. S.; Rantalainen, M.; Wilson, I. D. The metabonomics of aging and development in the rat: an investigation into the effect of age on the profile of endogenous metabolites in the urine of male rats using 1H NMR and HPLC-TOF MS. *Mol. Biosyst.* **2005**, *1* (2), 166−75.
(26) Nishimura, N.; Zhang, J.; Abo, M.; Okubo, A.; Yamazaki, S. Application of capillary electrophoresis to the simultaneous determination of betaines in plants. *Anal. Sci.* **2001**, *17* (1), 103−6.
(27) Gavaghan McKee, C. L.; Wilson, I. D.; Nicholson, J. K. Metabolic phenotyping of nude and normal (Alpk:ApfCD, C57BL10J) mice. *J. Proteome Res.* **2006**, *5* (2), 378−84.
(28) Liberles, S. D. Trace amine-associated receptors are olfactory receptors in vertebrates. *Ann. N. Y. Acad. Sci.* **2009**, *1170*, 168−72.
(29) Dumas, M. E.; Barton, R. H.; Toye, A.; Cloarec, O.; Blancher, C.; Rothwell, A.; Fearnside, J.; Tatoud, R.; Blanc, V.; Lindon, J. C.; Mitchell, S. C.; Holmes, E.; McCarthy, M. I.; Scott, J.; Gauguier, D.; Nicholson, J. K. Metabolic profiling reveals a contribution of gut microbiota to fatty liver phenotype in insulin-resistant mice. *Proc. Natl. Acad. Sci. U. S. A.* **2006**, *103* (33), 12511−6.
(30) Hatch, M.; Gjymishka, A.; Salido, E. C.; Allison, M. J.; Freel, R. W. Enteric oxalate elimination is induced and oxalate is normalized in a mouse model of primary hyperoxaluria following intestinal colonization with Oxalobacter. *Am. J. Physiol.: Gastrointest. Liver Physiol.* **2011**, *300* (3), G461−9.
(31) Gong, D. W.; Murayama, N.; Yamazoe, Y.; Kato, R. Hepatic triiodothyronine sulfation and its regulation by growth hormone and triiodothyronine in rats. *J. Biochem.* **1992**, *112* (1), 112−6.
(32) Phipps, A.; Stewart, J.; Wright, B.; Wilson, I. Effect of diet on the urinary excretion of hippuric acid and other dietary-derived aromatics in rat. A complex interaction between diet, gut microflora and substrate specificity. *Xenobiotica* **1998**, *28* (5), 527−37.
(33) Wang, Z.; Klipfell, E.; Bennett, B. J.; Koeth, R.; Levison, B. S.; Dugar, B.; Feldstein, A. E.; Britt, E. B.; Fu, X.; Chung, Y. M.; Wu, Y.; Schauer, P.; Smith, J. D.; Allayee, H.; Tang, W. H.; DiDonato, J. A.; Lusis, A. J.; Hazen, S. L. Gut flora metabolism of phosphatidylcholine promotes cardiovascular disease. *Nature* **2011**, *472* (7341), 57−63.